Macromolecules

pubs.acs.org/Macromolecules Article

Survey of Catalysts for Frontal Ring-Opening Metathesis Polymerization

Benjamin A. Suslick, Katherine J. Stawiasz,‖ Justine E. Paul,‖ Nancy R. Sottos, and Jeffrey S. Moore*

Cite This: *Macromolecules* 2021, 54, 5117−5123 Read Online

ACCESS | Metrics & More | Article Recommendations | Supporting Information

ABSTRACT: Recent advances in frontal ring-opening metathesis polymerization (FROMP) have enabled the rapid and energy-efficient fabrication of high-performance and thermoset materials. The second-generation Grubbs complex [(SIMes)$RuCl_2(PCy_3)$] is the most exploited FROMP catalyst to date despite the availability of several other commercial variants. Changes in the nature of the catalytic species may provide potential advantages for controlling FROMP conditions, polymer microstructure, and monomer selectivities. Herein, nine catalysts are employed for the FROMP of dicyclopentadiene and ethylidene norbornene mixtures to generate copolymers, and the associated polymerization process parameters (front temperatures and velocities) are measured for each system. Dynamic mechanical analysis, differential scanning calorimetry, and quasistatic tensile testing reveal significant differences in the mechanical and material properties of the resultant polymers.

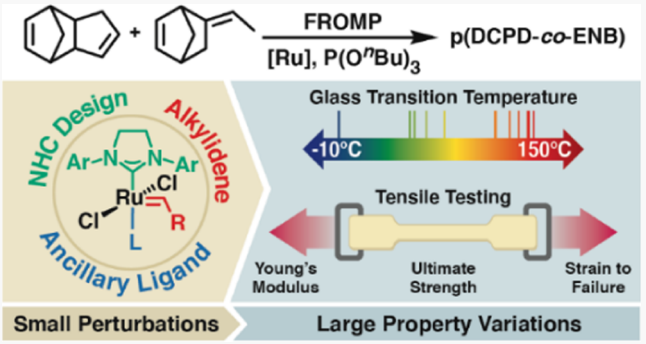

INTRODUCTION

Thermoset polymers and composites benefit numerous industrial-scale applications that require strong, stiff, and tough materials of low density.[1−5] Traditional curing methods involve prolonged heating and are limited by batchwise fabrication in high-temperature autoclaves for extended periods of time.[6−8] To improve energy efficiencies, reduce capital investment costs, and increase fabrication speed, a need exists for new, robust chemical processes that exploit the reaction enthalpy to self-sustain reactivity with minimal energy inputs.[9,10] Frontal ring-opening metathesis polymerization (FROMP) catalyzed by ruthenium complexes, such as first- or second-generation Grubbs catalysts, has emerged as an exciting catalytic platform relevant to several practical applications.[11−13] In FROMP, an initial thermal[11−17] (or photo)[18] stimulus initiates a polymerization event. The heat released from the catalytic ring opening of highly strained cyclic olefin monomers triggers subsequent catalytic events ahead of the reaction zone. The net process, therefore, involves a reaction zone that traverses through the monomer resin with a measurable steady-state velocity and a well-defined monomer-to-polymer interface.

Frontal polymerizations (FP) are predicated on minimal background reactivity prior to the triggering stimulus.[9,10] Under typical processing conditions, most metathesis catalysts react with strained olefinic monomers on a time scale fast enough to preclude reasonable storage times; the addition of catalyst to monomer resins induces spontaneous polymerization. One method to circumvent this involved the addition of inhibiting co-additives, as highlighted by work from the Pojman,[13] Mariani,[19,20] and Moore[11,12,15−17] groups. The addition of 100 ppm P(O^{n}Bu)$_3$ to a dicyclopentadiene (**DCPD**) resin with the commercially obtainable second-generation Grubbs catalyst (**Ru-1**, Chart 1), for example, extended the shelf life to nearly 30 h.[15] Similarly, the Mariani group[20] described the use of (R)-(+)-limonene as an inhibiting solvent, which provided resins with shelf-lives greater than 10 h at 20 mol % loadings.

Despite the versatility of **Ru-1** toward FROMP, other catalysts remain relatively unexplored; to date, all but one literature report employs **Ru-1** for FROMP.[11−21] Moreover, numerous advances in metathesis chemistry over the past decade have provided a plethora of commercially accessible catalysts.[22−25] The catalyst design can be tailored to match the specific needs desired, such as fast initiation, latent reactivity, and polymer microstructure (*e.g.*, *E*/*Z* ratio). The adaptation and implementation of such catalysts to FROMP, therefore, expands the available chemical space by providing an adjustable parameter to modify the physical and mechanical properties of frontally derived polymers. While typical bulk

Received: March 15, 2021
Revised: April 27, 2021
Published: May 17, 2021

https://doi.org/10.1021/acs.macromol.1c00566
Macromolecules 2021, 54, 5117−5123

Chart 1. FROMP Catalyst Formulations Tested in This Research[a]

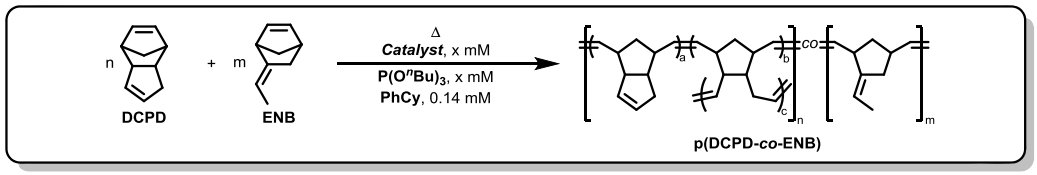

Catalyst	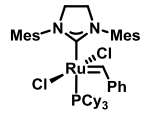 Ru-1	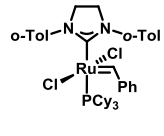 Ru-2	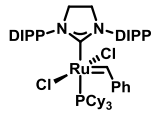 Ru-3	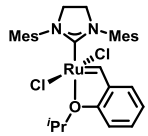 Ru-4	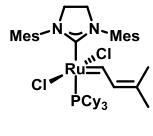 Ru-5
Catalyst Conc. (mM)	0.5	0.5	0.5	1.5	0.5
P(O^{n}Bu)$_3$ Conc. (mM)	0.5	0	0.5	4.5	2.0

Catalyst	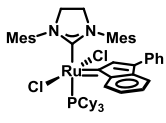 Ru-6	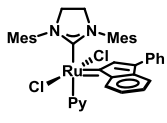 Ru-7	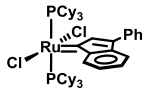 Ru-8	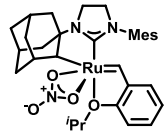 Ru-9
Catalyst Conc. (mM)	0.5	0.5	1.0	1.5
P(O^{n}Bu)$_3$ Conc. (mM)	0.5	0.5	0	0

[a]Catalytic formulation was comprised with the depicted catalysts and P(O^{n}Bu)$_3$ at the concentrations listed, with phenylcyclohexane (PhCy, 0.14 mM) as a solubilizing co-additive to achieve a total resin volume of 3 mL. Mes = 2,4,6-Me$_3$C$_6$H$_2$, *o*-Tol = 2-MeC$_6$H$_4$, DIPP = 2,6-^{i}Pr$_2$C$_6$H$_3$, Cy = C$_6$H$_{11}$, and Py = C$_5$H$_5$N.

metathesis studies are based on experiments below 100 °C, the FROMP reaction front reaches maximum temperatures of 200 °C and hotter. This fact, and the physicochemical complexities of transforming neat monomers into polymers and thermosets, requires an experimental investigation of catalyst activity under FROMP conditions. Here, we report polymerization and material observations following an exploratory, survey study.

RESULTS AND DISCUSSION

Formulation Design. Herein, we tested nine commercially available metathesis catalysts (**Ru-1** through **Ru-9**; Chart 1) for their FROMP activity. The chosen catalysts contained various *N*-heterocyclic carbene ligands (**Ru-1**, **-2**, **-3**), Schrock-type alkylidene fragments (**Ru-1**, **-4**, **-5**, **-6**), and ancillary ligands (**Ru-4**, **-6**, **-7**, **-8**). Additionally, a bis-chelating complex, **Ru-9**, was chosen due to its unique structure. While catalyst formulations were able to achieve stable frontal polymerization, their FROMP behaviors were markedly different.

Initial optimization for each new catalyst was performed in a monomer resin comprised of a 95:5 mixture of **DCPD** to 5-ethylidene-2-norbornene (**ENB**). All formulations included small quantities of phenylcyclohexane (PhCy) as a solubilizing co-additive. Recent work from our laboratories highlighted a solvent-free formulation with **Ru-1**, which requires extended sonication to achieve homogeneity.[17] While this method provides polymers with higher glass-transition temperatures, not all catalysts employed in this study are amenable to solvent-free conditions; in some cases, the poor solubility of the catalyst in neat resin precludes its usage for solvent-free FROMP. Catalyst and P(O^{n}Bu)$_3$ loadings were determined based on the minimum quantities required to support a stable front after thermal ignition with a soldering iron. Surprisingly, complex **Ru-9** decomposes in the presence of added phosphite ligand and could only provide fronts in the absence of an inhibiting reagent.[26]

Given these requirements, direct comparisons based solely on precatalyst structure are not straightforward, as the formulations did not consist of identical catalyst nor P(O^{n}Bu)$_3$ concentrations. Comparisons, therefore, must instead consider the identity of the entire formulation. Henceforth, the catalyst formulations are abbreviated by the identity of the catalyst, as given in Chart 1.

Frontal Process Parameters. The frontal parameters were determined for each catalytic formulation across a range of monomer compositions, which spanned **DCPD**/**ENB** volume ratios of 95:5 to 0:100 (see the Supporting Information, Figures S1−S9). Not all formulations, however, supported stable polymer fronts across this range of monomer ratios. We found that monomer compositions of **DCPD**/**ENB** in volume ratios of 60:40 supported well-defined reaction fronts for every catalytic formulation described in Chart 1. We selected this monomer composition to compare material properties that resulted from different catalyst formulations. Representative front videos (and select IR Thermographic footage) are found in the Supporting Information, Videos S1−S11.

The maximum front temperatures (T_{max}, Figure 1A) achieved during FROMP did not display a strong dependence on the choice of the catalytic formulation. Fronts derived from formulations **Ru-1** through **Ru-8** achieved T_{max} values in the range of 160−220 °C, regardless of the monomer composition (see the Supporting Information, Figures S1−S9). One notable exception occurred with fronts generated from **Ru-9**, which exhibited T_{max} values considerably lower than any of the other systems (ca. 100 °C) despite containing a higher catalyst concentration without added inhibitor. In contrast to the other catalysts, the T_{max} obtained by **Ru-9**-derived resins exhibited a

https://doi.org/10.1021/acs.macromol.1c00566
Macromolecules 2021, 54, 5117−5123

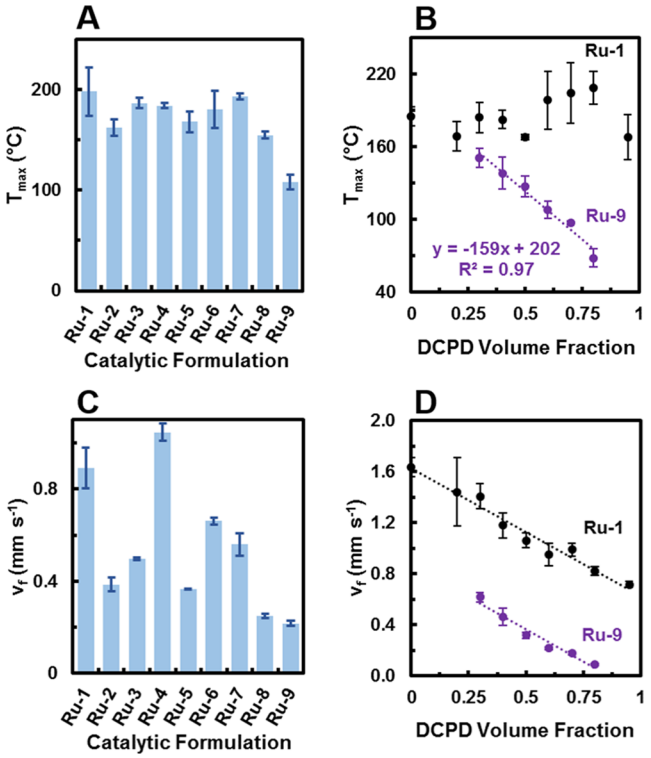

Figure 1. Frontal parameters for **DCPD**/**ENB** resin formulations **Ru-1** through **Ru-9**. All FROMP experiments are performed in 13 mm × 100 mm glass test tubes, and error bars are determined from the standard deviation of triplicate experiments. (A) Maximum front temperature (T_{max}) achieved by each new catalyst formulation during the FROMP of resins comprised of 60:40 **DCPD**/**ENB**, as measured by an embedded K-type thermocouple. (B) Linear dependence of monomer composition on T_{max} for **Ru-9**; in contrast, T_{max} achieved in systems **Ru-1** through **Ru-8** are invariant of the monomer composition. (C) Front velocity (ν_f) observed for each catalytic formulation at a **DCPD**/**ENB** volume ratio of 60:40. (D) All catalysts tested in this study exhibit a linear dependence of monomer composition on ν_f.

sharp inverse dependency on the volume ratio of **DCPD** to **ENB** (Figure 1B); resins with higher **DCPD** content polymerized at lower front temperatures than those primarily comprised of **ENB**.

The observed ν_f does not always exhibit a well-defined correlation to the catalyst structure, as depicted in Figure 1C. Increases in the steric bulk of the ancillary *N*-heterocyclic carbene ligand, for example, do not afford monotonic increases in ν_f (i.e., ν_f(**Ru-1**) > ν_f(**Ru-3**) > ν_f(**Ru-2**)). The effects imparted by changes in the Schrock-type carbene fragment, however, obey a general trend. Benzylidene-based precatalyst formulations (**Ru-1** and **Ru-4**) supported the fastest fronts (0.89 ± 0.09 and 1.05 ± 0.04 mm s^{-1}, respectively). In contrast, fronts derived from the analogous allylidene (**Ru-5**) and indenylidene (**Ru-6**) complexes propagated at slower speeds (0.37 ± 0.01 and 0.66 ± 0.01 mm s^{-1}, respectively), despite exhibiting nearly identical T_{max} values. The identity of the bottom-bound ligand primarily affects the degree to which undesired boiling occurs at the polymer front. Catalysis with the pyridine bound complex **Ru-7**, for example, proceeds with a visible generation of volatiles, unlike the analogous PCy_3 complex **Ru-6**, likely as the result of pyridine's low boiling point. The resultant void spaces generated from the production of volatiles dramatically weaken the associated mechanical properties. Similar to trends observed in cross-metathesis catalysis,[27] bis(phosphine) complexes are less active toward FROMP than the analogous *N*-heterocyclic carbene ligated species; **Ru-6** provided faster fronts than those observed with **Ru-8** (0.25 ± 0.01 mm s^{-1}). Curiously, cold fronts derived by **Ru-9** propagated with ν_f values (0.22 ± 0.01 mm s^{-1}) nearly identical to those observed for **Ru-8**, despite a nearly 50 °C difference in T_{max}.

Another key distinguishing feature among the catalytic systems is the temperature evolution as a function of time (see the Supporting Information, Figures S1A–S9A). At the thermocouple, the rate of temperature change ($\frac{dT}{dt}$, °C s^{-1}) provided insight into the broadness of the reaction front. An ideal polymerization front displays a sharp and narrow temperature gradient, as this ensures concurrent polymerization and cross-linking (i.e., curing); this corresponds to a Gaussian-like peak shape in the corresponding $\frac{dT}{dt}$ plot. Diffuse fronts, on the other hand, are problematic as catalysis occurs over a larger range of temperatures (i.e., inhomogeneity in temperature), which may impact the uniformity of corresponding mechanical properties. In this context, formulations **Ru-1**, **-2**, **-3**, **-4**, **-6**, and **-7** exhibited single, narrow peaks over ca. 5 s in the corresponding $\frac{dT}{dt}$ plots. Catalysis with **Ru-8**, in contrast, displayed a single broad temperature evolution over the span of ca. 20 s, which may result from its colder front temperatures.

Unlike the other catalytic systems, **Ru-5** and **Ru-9** exhibited two peaks in the $\frac{dT}{dt}$ plots, which suggests the existence of two reaction fronts during FROMP. For **Ru-5**, the first, colder front existed in close spatiotemporal proximity to the hotter, second front (see the Supporting Information, Figure S5A). In contrast, **Ru-9** exhibited two exceedingly broad temperature evolution events over the course of ca. 60 s. Indeed, this is directly observed in the thermographic video for **Ru-9** at a **DCPD**/**ENB** volume ratio of 60:40 (see the Supporting Information, Video S11).

Unlike T_{max}, the front velocities (ν_f) were inversely dependent on the **DCPD** volume fraction for all of the catalytic formulations tested (Figure 1D and Supporting Information, Figures S1–S9). Only the absolute values of ν_f varied with the identity of the catalytic system. At this time, it is unclear whether a direct correlation between T_{max} and ν_f exists, and continued research efforts are underway to explore this further.

Initiation of FROMP occurred reasonably quickly (ca. <1 min) for each of the formulations tested. In general, formulations containing benzylidene-derived catalysts (**Ru-1** through **Ru-4** and **Ru-9**) rapidly initiate (<10 s) after localized contact heating by soldering iron. In contrast, the allylidene (**Ru-5**) and indenylidene (**Ru-6** through **Ru-8**) formulations require prolonged heating prior to the front formation (ca. 20–40 s).

Resin Stability and Storage Lifetime. The catalyst identity dictates the stability and storability of the resin and influences the adaptation of FROMP to large-scale, applications. Potlife is the term used in FP to describe the processing window for a resin, and several different definitions exist in the literature.[11,19] Our laboratories typically define potlife as the time required for the resin to reach a gel-like state incapable of sustaining a propagating front (i.e., the point at which front quenching occurs).[11] In contrast, the Mariani group[19] defines

https://doi.org/10.1021/acs.macromol.1c00566
Macromolecules 2021, 54, 5117–5123

potlife as the maximum length of time that a resin remains viable for frontal polymerization prior to spontaneous polymerization (or alternatively as the length of time prior to sudden temperature increases due to background polymerization). These definitions highlight two different modes of failure in FP: front quenching and spontaneous polymerization. Additionally, potlife typically does not consider the volume of resin or the dimensionality of the storage vessel, which are key parameters for successful FP. The volume-to-surface area ratio dictates the rate of heat loss from the reaction front and can influence front-quenching or autoacceleration phenomena. Given these considerations, we favor the use of a rigorously defined parameter, storage lifetime (t_s), to describe the processing window of each catalytic formulation. We define t_s as the maximum length of time 30 mL of catalyst-containing resin (stored in a 40 mL scintillation vial at ambient temperatures) remains viable for FROMP without significant change (> 25%) to the observed T_{max} or ν_f. Mixtures stored after the t_s have undergone a significant degree of background polymerization and are no longer able to generate sufficient heat to sustain a stable FP reaction (i.e., depressed T_{max} and ν_f). Resins that undergo spontaneous polymerization also possess measurable t_s, after which ν_f rapidly accelerates. When fabrication requires a long processing window, catalyst-resin mixtures must exhibit sufficiently long t_s values to enable scalable applications.

Several key considerations exist when analyzing and contrasting t_s values. Direct comparisons based solely on catalyst structure, for example, are highly problematic as many systems required different concentrations of $P(O^nBu)_3$ to support stable polymer fronts. Prior reports have demonstrated that increases in inhibitor concentration prolong the potlife of **Ru-1**-based resins, albeit at the retardation of the associated ν_f.[15] Additionally, the catalytic formulation influences two separate reaction manifolds relevant for stable FP, each with different associated kinetics: catalyst activation and polymer propagation. A subtle mixture of these two reaction types dictates the storage lifetime; catalysts that induce rapid polymer propagation, for example, may exhibit extended storage lifetimes if the prerequisite catalyst activation occurs slowly.

The differences in the measured t_s values highlight the most obvious and relevant differences among the catalytic systems tested (Figure 2). Each formulation exists in one of three distinct lifetime regimes: short, intermediate, and long. Successful FP of resins with short t_s (i.e., **Ru-2**, **-3**, **-6**, **-8**, and **-9**) requires immediate initiation (<5 min) to avoid spontaneous polymerization; applications with these catalytic mixtures, therefore, may require further optimization (e.g., more inhibitor) to extend the processing window. Alternatively, background polymerization suppression occurs at reduced temperatures, so more desirable t_s may exist with chilled resins, but this was not explored in detail here. Intermediate lifetimes (ca. 1−6 h) exist for catalysis with **Ru-1**, **-4**, and **-7**, despite supporting fronts with vastly different ν_f. After initiation, fronts derived from **Ru-4** undergo propagation at a faster rate than **Ru-7**. The similarity in storage lifetime, therefore, appears to relate to the difference in catalyst activation kinetics, rather than the rates of propagation. Indeed, this is best observed in the difference between **Ru-1** and **Ru-5**. The allylidene precatalyst **Ru-5** displayed the longest storage lifetime (ca. 36 h) despite its structural similarity to **Ru-1**. While the active species for both systems are identical after the first turnover, the rates with which these catalysts activate are different.[27]

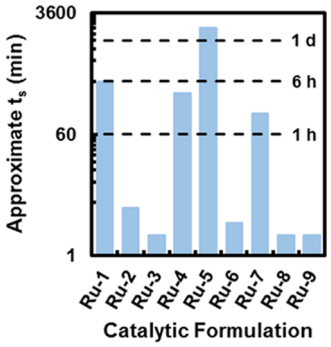

Figure 2. Approximate storage lifetimes (t_s) for resins comprised of **Ru-1** through **Ru-9** at **DCPD**/**ENB** volume ratios of 60:40. The t_s values are approximated as the length of time that the mixed catalyst/monomer resin is viable for FP at ambient temperatures prior to spontaneous polymerization.

Mechanical Properties of Frontally Derived Polymers.

To investigate the mechanical property differences of the polymers derived from the various catalytic systems, we employed quasistatic tensile testing and dynamic mechanical analysis (DMA; Table 1). Polymer swell tests were also performed for each system, and are described in detail in the Supporting Information (Tables S8 and S9 and Figures S10−S19). Tensile tests provided the elastic modulus (E), yield strength, and fracture strain of each polymer. The specific catalyst formulation only slightly influenced the stress−strain behavior of the resultant polymer in most cases. Copolymers derived from **Ru-1** through **Ru-8** at a **DCPD**/**ENB** volume ratio of 60:40, for example, exhibited E values in the range of 1.3−1.6 GPa (Table 1). Indeed, these values match reasonably well with those observed for other highly cross-linked, frontally derived p(**DCPD**) copolymers;[11,17] this similarity is also borne out in the ultimate tensile strengths (ca. 25−50 MPa) and fracture strains (ca. 5%) of these copolymers, as observed in Table 1. In great contrast, polymers derived from catalyst **Ru-9** at a **DCPD**/**ENB** volume ratio of 60:40 displayed exceedingly unusual nonlinear stress−strain properties, with a Young's modulus (20 ± 10 MPa) and ultimate tensile strength (1.1 ± 0.1 MPa) nearly 2 orders of magnitude smaller than those observed with **Ru-1** through **Ru-8**. Additionally, the **Ru-9**-derived polymer exhibited an apparent yield point (0.62 MPa) separate from its ultimate tensile strength (see the Supporting Information, Figure S23). This polymer is unable to bear the same applied loads typically accessible for the copolymers prepared by most catalysts; indeed, the copolymer derived from **Ru-9** behaves like an elastomeric material, as indicated by the large fracture strain value (143%).

We then employed DMA experiments to investigate thermomechanical properties. The glass-transition temperatures (T_g) for polymers derived from each catalytic system were determined as the maxima of the ratio of the E''/E', known as tan δ. Typical T_g values for p(**DCPD**) derived from **Ru-1** exist in the range of 120−160 °C as described in previous literature reports;[15,17,18,21] moreover, these values are highly dependent on the specific resin formulation, such as solvent choice or monomer composition. Indeed, we observe a T_g of 126 ± 1 °C for a 60:40 mixture of **DCPD**/**ENB** with **Ru-1** (Table 1), which is in good agreement with these earlier

https://doi.org/10.1021/acs.macromol.1c00566
Macromolecules 2021, 54, 5117−5123

Table 1. Mechanical Properties of Frontally Derived Polymers Ru-1 through Ru-9 at a DCPD/ENB Volume Ratio of 60:40

catalytic formulation	E (GPa)	ultimate tensile strength (MPa)	failure strain (%)	transition temperatures (°C)
Ru-1	1.58 ± 0.06	47 ± 2	5.0 ± 1.0	126 ± 1
Ru-2[a]	1.45 ± 0.06	32 ± 2	2.9 ± 0.3	50 ± 5/119 ± 3
Ru-3	1.44 ± 0.04	44 ± 2	5.8 ± 0.4	105 ± 8
Ru-4	1.52 ± 0.06	48 ± 2	5.2 ± 0.7	130 ± 1
Ru-5[a]	1.50 ± 0.09	33 ± 1	2.5 ± 0.2	59 ± 2/105 ± 6
Ru-6	1.60 ± 0.05	40 ± 1	3.5 ± 0.8	126 ± 2
Ru-7	1.48 ± 0.04	36 ± 2	3.1 ± 0.5	114 ± 2
Ru-8	1.30 ± 0.15	28 ± 2	2.9 ± 0.1	47 ± 5
Ru-9[a]	0.02 ± 0.01	1.1 ± 0.1	143 ± 4	1 ± 1/70 ± 1

[a]Samples displayed two distinct peaks in the tanδ plot calculated from the DMA experiment (see Figure 3). For representative plots, see the Supporting Information, Figures S20−S23.

reports. Copolymers produced by FROMP with complexes **Ru-3**, **-4**, **-6**, and **-7** exhibited similar T_g values (ca. 100−130 °C). It is unsurprising that these values exist on the low end of the reported temperature range as the addition of **ENB** to the resin reduces the potential for cross-linking, thereby lowering the observed T_g.

Intriguingly, several formulations provided polymers with unusual temperature-dependent transition properties. Polymers produced by the bis(phosphine) complex **Ru-8** at a 60:40 **DCPD/ENB** volume ratio (Table 1 and Figure 3A), for example, display markedly lower T_g values (47 ± 5 °C) than the analogous *N*-heterocyclic carbene containing counterpart, **Ru-6** (126 ± 2 °C). The catalyst structure appears to play an important role in dictating the transition behavior, although the specific mechanism for the observed difference in T_g is not known at present.

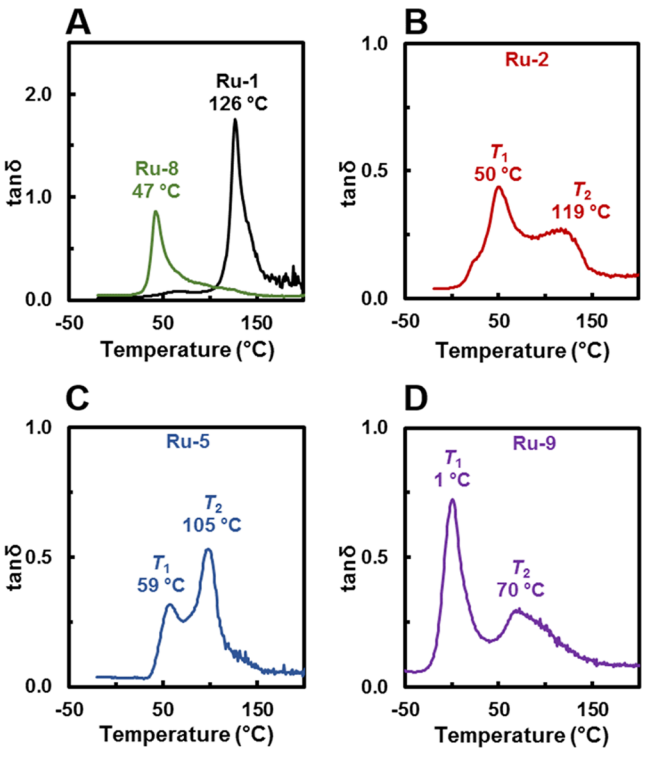

Figure 3. Representative temperature dependence of tan δ for test samples comprised of **DCPD/ENB** volume ratios of 60:40 for polymers derived from catalysts **Ru-1** and **Ru-8** (A), **Ru-2** (B), **Ru-5** (C), and **Ru-9** (D). The peaks in the tan δ plots of (A) correspond to glass-transition temperatures; at present, the physical processes involved in samples with two transitions (B−D) are unclear. Representative tan δ plots for all catalytic systems are found in the Supporting Information, Figures S20−S22.

Catalysis with **Ru-2**, **Ru-5**, and **Ru-9** provided copolymers with two characteristic transition temperature values (Figure 3B−D) at **DCPD/ENB** volume ratios of 60:40; with **Ru-2** and **Ru-5**, the second, higher temperature transition (T_2) occurs in a similar range to those observed with copolymers with a single peak in tan δ (Figure 3B,C). The lower temperature transition (T_1) occurs at ca. 50−60 °C. In contrast, the observed transitions for **Ru-9** occur at significantly lower temperatures (1 and 70 °C; Figure 3D) despite being fully cured, as determined by the lack of an exothermic event in the first thermal scan of a postcure DSC analysis. This suggests that the temperature-dependent mechanical properties of **Ru-9**-derived copolymers do not result from incomplete monomer consumption, and instead are an intrinsic property related to the polymers derived from this catalytic system.

The second heating scan of the postcure DSC for the polymers derived from **Ru-2**, **Ru-5**, and **Ru-9** confirmed the existence of multiple transition temperatures (see the Supporting Information, Figures S24−S26); these values were in good agreement with those determined by DMA (within ± 20 °C). While the specific microstructural and morphological causes for the two observed transitions are not known at present, precedence exists in other copolymerization systems.[28,29] Daimon et al.[28] described the glass-transition properties of styrene/cyclododecyl acrylate copolymers as a function of the copolymer structure (i.e., random, blocky, or blend of homopolymers). Randomly distributed copolymers exhibited single T_g values as the weighted average of the two homopolymers as described by the Wood equation. In contrast, blocky or blended copolymers exhibited two transition temperatures that matched the T_g values of each homopolymer. Indeed, similar behavior is observable by DMA, as outlined by Kraus and co-workers;[29] randomly distributed copolymers of butadiene and styrene exhibited a single tan δ peak, whereas ideal blocky structures displayed two characteristic transition features. It is possible, therefore, that the observed transition temperatures in our work with polymers derived from **Ru-2**, **Ru-5**, and **Ru-9** at a **DCPD/ENB** volume ratio of 60:40 result from a blocky morphology or from a blend of the corresponding homopolymers. Concurrent investigations into the mechanistic cause for these unusual thermomechanical properties are underway.

https://doi.org/10.1021/acs.macromol.1c00566
Macromolecules 2021, 54, 5117−5123

CONCLUSIONS

This study evaluated the process parameters for nine catalytically competent frontal ring-opening metathesis polymerization (FROMP) formulations. Specifically, the chosen commercially available catalysts contain a common organometallic scaffold based on a ruthenium alkylidene motif, as well as added phosphite inhibitor. The FP parameters (e.g., T_{max} and v_f) and material properties of the resultant polymers (e.g., T_g and E) were ascertained for each catalytic system across a range of monomer compositions. The choice of formulation did not have a significant effect on the temperatures with which FROMP occurs. In contrast, the velocity of the traversing reaction front is highly dependent on the specific catalytic composition. Significantly, formulations comprised of a catalyst bearing an allylidene fragment (**Ru-5**) exhibit long storage lifetimes (ca. 36 h), which may result from an increased resistance to background polymerization reactivity.

The material properties of the final polymer depend on the catalyst employed; specifically, T_g varies among the different catalytic systems, despite containing an identical monomer composition. Many formulations provided T_g values in the range of 110−130 °C, consistent with previous literature reports.[15,17,18,21] Several formulations, however, provided copolymers with multiple transition features over a broad temperature range (ca. 0−120 °C). While the exact mechanism for the observed behavior is not known, differences in the catalyst ligand sphere (e.g., sterics) or polymerization kinetics likely influence the polymer microstructure and the associated mechanical properties. Notably, formulations comprised of **Ru-9** provided uniquely elastomeric p(**DCPD**), characterized by a low Young's modulus and large strain at failure value. The results from this study highlight an often-overlooked facet of polymerization engineering: small perturbations to the catalyst identity result in a substantial variance in final product properties.

ASSOCIATED CONTENT

Supporting Information

The Supporting Information is available free of charge at https://pubs.acs.org/doi/10.1021/acs.macromol.1c00566.

Experimental details; frontal process parameters; and polymer characterization data (PDF)
Video S1: representative front (Ru-1) (MP4)
Video S2: representative front (Ru-2) (MP4)
Video S3: representative front (Ru-3) (MP4)
Video S4: selected IR thermographic (Ru-3 Thermographic) (MP4)
Video S5: representative front (Ru-4) (MP4)
Video S6: representative front (Ru-5) (MP4)
Video S7: representative front (Ru-6) (MP4)
Video S8: representative front (Ru-7) (MP4)
Video S9: representative front (Ru-8) (MP4)
Video S10: representative front (Ru-9) (MP4)
Video S11: selected IR thermographic (Ru-9 Thermographic) (MP4)

AUTHOR INFORMATION

Corresponding Author

Jeffrey S. Moore − *Beckman Institute for Advanced Science and Technology, University of Illinois at Urbana−Champaign, Urbana, Illinois 61801, United States; Department of Chemistry, University of Illinois at Urbana−Champaign, Urbana, Illinois 61801, United States;* Email: jsmoore@illinois.edu

Authors

Benjamin A. Suslick − *Beckman Institute for Advanced Science and Technology, University of Illinois at Urbana−Champaign, Urbana, Illinois 61801, United States; Department of Chemistry, University of Illinois at Urbana−Champaign, Urbana, Illinois 61801, United States*

Katherine J. Stawiasz − *Beckman Institute for Advanced Science and Technology, University of Illinois at Urbana−Champaign, Urbana, Illinois 61801, United States; Department of Chemistry, University of Illinois at Urbana−Champaign, Urbana, Illinois 61801, United States;* orcid.org/0000-0003-2518-0557

Justine E. Paul − *Beckman Institute for Advanced Science and Technology, University of Illinois at Urbana−Champaign, Urbana, Illinois 61801, United States; Department of Materials Science and Engineering, University of Illinois at Urbana−Champaign, Urbana, Illinois 61801, United States*

Nancy R. Sottos − *Beckman Institute for Advanced Science and Technology, University of Illinois at Urbana−Champaign, Urbana, Illinois 61801, United States; Department of Materials Science and Engineering, University of Illinois at Urbana−Champaign, Urbana, Illinois 61801, United States;* orcid.org/0000-0002-5818-520X

Complete contact information is available at: https://pubs.acs.org/10.1021/acs.macromol.1c00566

Author Contributions

‖K.J.S. and J.E.P. contributed equally to this paper.

Notes

The authors declare no competing financial interest.

ACKNOWLEDGMENTS

This work was primarily funded by Air Force Office of Scientific Research under award number FA9550-20-1-0194 and the National Science Foundation under award number NSF CMMI 19-33932. K.J.S. acknowledges the U.S. Department of Defense for an NDSEG Fellowship. J.E.P. acknowledges the Beckman Institute at the University of Illinois, Urbana-Champaign for a graduate fellowship. Drs. Diego Alzate-Sanchez, William Neary, and Julian Cooper are thanked for insightful discussions.

REFERENCES

(1) Brøndsted, P.; Lilholt, H.; Lystrup, A. Composite Materials for Wind Power Turbine Blades. *Annu. Rev. Mater. Res.* **2005**, *35*, 505−538.
(2) Karbhari, V. M.; Seible, F. Fiber Reinforced Composites − Advanced Materials for the Renewal of Civil Infrastructure. *Appl. Compos. Mater.* **2000**, *7*, 95−124.
(3) Timmis, A. J.; Hodzic, A.; Koh, L.; Bonner, M.; Soutis, C.; Schäfer, A. W.; Dray, L. Environmental Impact Assessment of Aviation Emission Reduction through the Implementation of Composite Materials. *Int. J. Life Cycle Assess.* **2015**, *20*, 233−243.
(4) Friedrich, K.; Almajid, A. A. Manufacturing Aspects of Advanced Polymer Composites for Automotive Applications. *Appl. Compos. Mater.* **2013**, *20*, 107−128.
(5) Giurgiutiu, V. *Introduction in Structural Health Monitoring of Aerospace Composites*; Giurgiutiu, V., Ed.; Academic Press: Oxford, 2016; Chapter 1, pp 1−23.

(6) Abliz, D.; Duan, Y.; Steuernagel, L.; Xie, L.; Li, D.; Ziegmann, G. Curing Methods for Advanced Polymer Composites - a Review. *Polym. Polym. Compos.* **2013**, *21*, 341−348.
(7) Bachmann, J.; Hidalgo, C.; Bricout, S. Environmental Analysis of Innovative Sustainable Composites with Potential Use in Aviation Sector—a Life Cycle Assessment Review. *Sci. China Technol. Sci.* **2017**, *60*, 1301−1317.
(8) Pascault, J.-P.; Sautereau, H.; Verdu, J.; Williams, R. J. J. *Thermosetting Polmers*; CRC Press: New York, NY, USA, 2002.
(9) Pojman, J. A.; Ilyashenko, V. M.; Khan, A. M. Free-Radical Frontal Polymerization: Self-Propagating Thermal Reaction Waves. *J. Chem. Soc., Faraday Trans.* **1996**, *92*, 2825−2837.
(10) Pojman, J. A. Frontal Polymerization. In *Polymer Science: A Comprehensive Reference*; Matyjaszewski, K.; Möller, M., Eds.; Elsevier: Amsterdam, 2012; pp 957−980.
(11) Robertson, I. D.; Yourdkhani, M.; Centellas, P. J.; Aw, J. E.; Ivanoff, D. G.; Goli, E.; Lloyd, E. M.; Dean, L. M.; Sottos, N. R.; Geubelle, P. H.; Moore, J. S.; White, S. R. Rapid Energy-Efficient Manufacturing of Polymers and Composites Via Frontal Polymerization. *Nature* **2018**, *557*, 223−227.
(12) Dean, L. M.; Wu, Q.; Alshangiti, O.; Moore, J. S.; Sottos, N. R. Rapid Synthesis of Elastomers and Thermosets with Tunable Thermomechanical Properties. *ACS Macro Lett.* **2020**, *9*, 819−824.
(13) Mariani, A.; Fiori, S.; Chekanov, Y.; Pojman, J. A. Frontal Ring-Opening Metathesis Polymerization of Dicyclopentadiene. *Macromolecules* **2001**, *34*, 6539−6541.
(14) Liu, H.; Wei, H.; Moore, J. S. Frontal Ring-Opening Metathesis Copolymerization: Deviation of Front Velocity from Mixing Rules. *ACS Macro Lett.* **2019**, *8*, 846−851.
(15) Robertson, I. D.; Dean, L. M.; Rudebusch, G. E.; Sottos, N. R.; White, S. R.; Moore, J. S. Alkyl Phosphite Inhibitors for Frontal Ring-Opening Metathesis Polymerization Greatly Increase Pot Life. *ACS Macro Lett.* **2017**, *6*, 609−612.
(16) Robertson, I. D.; Pruitt, E. L.; Moore, J. S. Frontal Ring-Opening Metathesis Polymerization of Exo-Dicyclopentadiene for Low Catalyst Loadings. *ACS Macro Lett.* **2016**, *5*, 593−596.
(17) Ivanoff, D. G.; Sung, J.; Butikofer, S. M.; Moore, J. S.; Sottos, N. R. Cross-Linking Agents for Enhanced Performance of Thermosets Prepared Via Frontal Ring-Opening Metathesis Polymerization. *Macromolecules* **2020**, *53*, 8360−8366.
(18) Stawiasz, K. J.; Paul, J. E.; Schwarz, K. J.; Sottos, N. R.; Moore, J. S. Photoexcitation of Grubbs' Second-Generation Catalyst Initiates Frontal Ring-Opening Metathesis Polymerization. *ACS Macro Lett.* **2020**, *9*, 1563−1568.
(19) Ruiu, A.; Sanna, D.; Alzari, V.; Nuvoli, D.; Mariani, A. Advances in the Frontal Ring Opening Metathesis Polymerization of Dicyclopentadiene. *J. Polym. Sci., Part A: Polym. Chem.* **2014**, *52*, 2776−2780.
(20) Alzari, V.; Nuvoli, D.; Sanna, D.; Ruiu, A.; Mariani, A. Effect of Limonene on the Frontal Ring Opening Metathesis Polymerization of Dicyclopentadiene. *J. Polym. Sci., Part A: Polym. Chem.* **2016**, *54*, 63−68.
(21) Dean, L. M.; Ravindra, A.; Guo, A. X.; Yourdkhani, M.; Sottos, N. R. Photothermal Initiation of Frontal Polymerization Using Carbon Nanoparticles. *ACS Appl. Polym. Mater.* **2020**, *2*, 4690−4696.
(22) Ogba, O. M.; Warner, N. C.; O'Leary, D. J.; Grubbs, R. H. Recent Advances in Ruthenium-Based Olefin Metathesis. *Chem. Soc. Rev.* **2018**, *47*, 4510−4544.
(23) Keitz, B. K.; Endo, K.; Patel, P. R.; Herbert, M. B.; Grubbs, R. H. Improved Ruthenium Catalysts for Z-Selective Olefin Metathesis. *J. Am. Chem. Soc.* **2012**, *134*, 693−699.
(24) Herbert, M. B.; Suslick, B. A.; Liu, P.; Zou, L.; Dornan, P. K.; Houk, K. N.; Grubbs, R. H. Cyclometalated Z-Selective Ruthenium Metathesis Catalysts with Modified N-Chelating Groups. *Organometallics* **2015**, *34*, 2858−2869.
(25) Monsaert, S.; Lozano Vila, A.; Drozdzak, R.; Van Der Voort, P.; Verpoort, F. Latent Olefin Metathesis Catalysts. *Chem. Soc. Rev.* **2009**, *38*, 3360−3372.
(26) Herbert, M. B.; Lan, Y.; Keitz, B. K.; Liu, P.; Endo, K.; Day, M. W.; Houk, K. N.; Grubbs, R. H. Decomposition Pathways of Z-Selective Ruthenium Metathesis Catalysts. *J. Am. Chem. Soc.* **2012**, *134*, 7861−7866.
(27) Sanford, M. S.; Love, J. A.; Grubbs, R. H. Mechanism and Activity of Ruthenium Olefin Metathesis Catalysts. *J. Am. Chem. Soc.* **2001**, *123*, 6543−6554.
(28) Daimon, H.; Okitsu, H.; Kumanotani, J. Glass Transition Behaviors of Random and Block Copolymers and Polymer Blends of Styrene and Cyclododecyl Acrylate. I. Glass Transition Temperatures. *Polym. J.* **1975**, *7*, 460−466.
(29) Kraus, G.; Childers, C. W.; Gruver, J. T. Properties of Random and Block Copolymers of Butadiene and Styrene. I. Dynamic Properties and Glassy Transition Temperatures. *J. Appl. Polym. Sci.* **1967**, *11*, 1581−1591.

https://doi.org/10.1021/acs.macromol.1c00566
Macromolecules 2021, 54, 5117−5123